On the Comparative Performance Analysis of Turbo-Coded Non-Ideal Single-Carrier and Multi-Carrier Waveforms over Wideband Vogler-Hoffmeyer HF Channels

F. Genç*, M. A. Reşat*, A. Yavanoğlu*, and Ö. Ertuğ*
*
Gazi University
Telecommunications and Signal Processing Laboratory
Electrical and Electronics Engineering Department
Ankara, TURKEY

***Abstract*—The purpose of this paper is to compare the turbo-coded orthogonal frequency division multiplexing (OFDM) and turbo-coded single carrier frequency domain equalization (SC-FDE) systems under the effects of carrier frequency offset (CFO), symbol timing offset (STO) and phase noise in wideband Vogler-Hoffmeyer HF channel model. The BER performance versus CFO, STO and phase noise obtained through Monte-Carlo simulations shows that non-ideal turbo-coded OFDM has better performance with greater diversity than non-ideal turbo-coded SC-FDE system in wideband HF channel under Minimum Mean Square Error (MMSE) based channel estimation/equalization and cyclic-prefix based maximum-likekihood synchronization for CFO and STO.**

I. Introduction

Spectral and power efficiency of terminal in the limited bandwidth and transmit power have been developing continously for the new generation of wireless communication systems. To meet the new user demands new air interfaces are needed to be enhanced. Orthogonal Frequency-Division Multiplexing (OFDM) is a popular modulation technique to satisfy these requirements, adopted to broadcast systems, such as Digital Video Broadcasting (DVB), Digital Audio Broadcasting (DAB), Wireless Local Area Networks (WLAN) and Asymetric Digital Subcriber Line (ADSL) for wired systems. In OFDM systems, one Inverse Fast-Fourrier Transform (IFFT) block is used at the transmitter and also one FFT block is used at the receiver sides of the link. In the IFFT block, OFDM transmitter multiplexes the information into many low-rate streams which are transmitted parallelly instead of sending the information as a single stream [1]. The modulated signals in an OFDM system have high peak values in time domain since many subcarriers are added via an IFFT operation. Therefore, OFDM systems are known to have high Peak-to-Average Power Ratio (PAPR). Due to the limited battery life in mobile terminals, the PAPR problem is a main disadvantage of the OFDM system for the uplink.

On the other hand, Single-Carrier Frequency-Domain Equalization (SC-FDE) is a desirable alternative to OFDM systems. In the case of SC-FDE technique, no IFFT and FFT blocks existed at the transmit side while FFT and IFFT operators are performed at the receiver side of the link. SC-FDE experiences lower PAPR levels than OFDM because no IFFT is performed at the transmitter to precode the signal. In order to mitigate the PAPR problem, Single-Carrier (SC) transmission uses single-carrier modulation instead of many sub-carriers [1-3].

Low-complexity channel equalization and estimation in the frequency-domain are used to mitigate the inter-symbol interference (ISI) [4]. For this purpose, frequency domain MMSE equalizer is in generally used to minimize the attenuations of the fading channel. For wideband channels, conventional time domain equalizers are impractical because of the very long channel impulse response in the time domain. Frequency domain equalization is more practical for such channels because the DFT size does not grow linearly with the length of the channel response and the complexity of the FDE is much lower than the time domain equalizer.

At the same time, frequency domain MMSE estimation is prefered with the comb-type pilot tone arrangement to predict the multi-path channel coefficients [9-11]. In order to estimate the channel characteristics, the comb-type pilot symbols are placed as periodically as possible in coherence time. The coherence time is the inverse of the Doppler spread in the channel.

An additional way to eliminate ISI almost completely, is to use a guard interval which is called cyclic-prefix (CP). The CP is the replica of the last L symbols of the block as shown in Fig. 4. The guard time L must be larger than the expected channel delay spread. At the receiver, the received CP is discarded before processing the block. By doing so CP also prevents inter-block interference.

CP is also used in CP-based channel synchronization to compansate the inter-carrier interference (ICI) caused by the Doppler effect. CP-based synchronization enables CFO estimation without need of additional redundant pilots. In fact, the

key point is that CP already contains sufficient information to perform synchronization. Without CFO, the subchannels do not interfere with one another. The impact of frequency offset is loss of orthogonality between the tones. Hence, the received signal is not a white process because of its probabilistic structure and it contains information about the timing offset and carrier frequency offset [12]. Estimations of timing offset θ and frequency offset $\hat{\varepsilon}$ are achieved by the relation of the CPs of consecutive frames.

In this paper, the performances of the turbo-coded SC-FDE and OFDM systems in wideband Vogler-Hoffmeyer HF channels are compared. In practice, a wideband radio channel has time-variant, frequency-selective and noisy properties. Most commonly used HF channel model is recommended by CCIR and ITU-R that is called as Watterson HF channel [5,6]. The main restriction of the Watterson model is that the model is designed and tested for narrowband channels but not for ones having more than 12KHz bandwidth. In the design of high data speed wideband HF communication systems, exact modeling and simulation of HF channel are needed. Therefore, Vogler-Hoffmeyer HF channel model is used in this paper [7,8].

The remainder of this paper is organized as follows. Section II. gives an overview of the wideband Vogler-Hoffmeyer HF channel model. Section III. overviews OFDM and SC-FDE structures. In Section IV., channel equalization/estimation and synchronization methods are defined in detail. Numerical results and discussions are given in Section V. and finally, conclusions are drawn out from the results in Section VI.

II. Wideband HF Channel Model

HF channel characteristics are directly shaped by the ionosphere behavior because HF channels utilize the ionospheric reflections in order to provide long-distance communications.

The wideband HF channel can be modelled as a FIR filter where the taps are time-variant and have complex values. This model can be described by the following equation:

$$y_t = \sum_{i=0}^{L-1} h_i x_t + n_i \tag{1}$$

where y_t is the complex output of the channel, L is the length of the channel, h_i is one of the L taps of the time-varying transversal filter, x_t is the complex input to the channel and n_i is Additive White Gaussian Noise (AWGN).

This type of a complex-valued FIR filter can be formed easily by convolving the input signal with the channel impulse response. Thus, the coefficients of the filter can be defined as the samples of the HF channel impulse response which is given as:

$$h(t,\tau) = \sqrt{P(\tau)} D(t,\tau) \psi(t,\tau) \tag{2}$$

where $P(\tau)$ is the delay power profile, and its square root $\sqrt{P(\tau)}$ describes the shape in delay dimension; $D(t,\tau)$ is the deterministic phase function showing each path's Doppler shift, and $\psi(t,\tau)$ is the stochastic modulation function which describes the fading value of the impulse response.

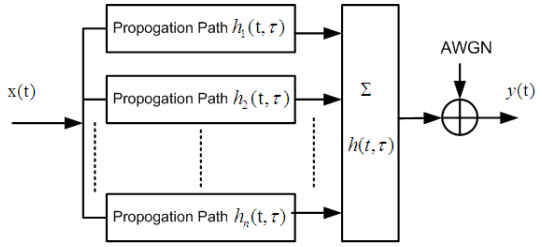

Fig. 1. HF Channel Model

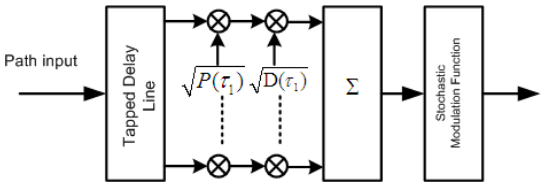

Fig. 2. Single Propagation Path

The Doppler Effect can also be given with the formula:

$$D(t,\tau) = e^{j2\pi f_D t} \tag{3}$$

where f_D is the Doppler shift value. The stochastic modulation function $\psi(t,\tau)$ can be stated as random variables with an autocorrelation function that possesses a Gaussian shape.

Whilst Fig. 1 shows the structure of the wideband HF channel model with propogation paths, Fig. 2 shows the model of a single propogation path [8]. It is important to specify the main difference between the narrowband Watterson model and the wideband channel model here. In the Watterson model time delay spread is neglected and the time delay of each path has a single value. On the other hand, the wideband model has a delay power profile symbolized with $P(\tau)$ and relates Doppler effect with the time delay of each path.

III. System Models

A. OFDM System

In this section, OFDM system model is illustrated in Fig. 3. First, each binary source datas are encoded by non-punctered, $R = 1/3$ code-rate turbo encoder and Log-Map

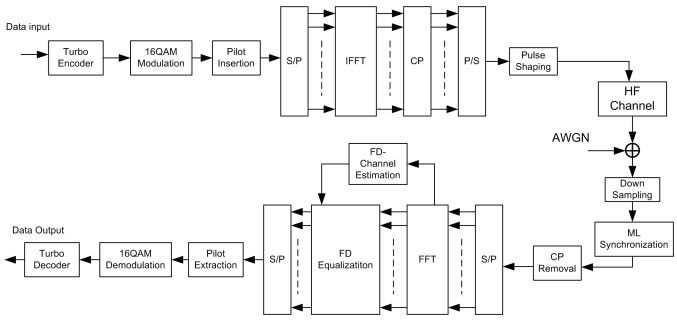

Fig. 3. OFDM Structure

algorithm is choosen for best decoding performance with low-complexity for turbo decoder. In this time, N subcarriers X_k for k=0,1,....N-1 are modulated by a signal alphabet $A = \{\pm 1, \pm 3, \pm j, \pm 3j\}$ used for transmitting the information for 16-QAM. After baseband modulation, pilot tone symbol insertion is applied for the channel estimation where the pilot pattern is shown in Fig. 4.

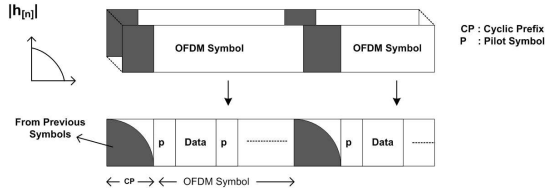

Fig. 4. Frame Structure

Pilot arrangement in OFDM system issue is discussed in more detail under the Section IV. Here, output of the IDFT after the serial to parallel conversion can be expressed as:

$$x(n) = \frac{1}{\sqrt{N}} \sum_{k=0}^{N-1} X(k) e^{j2\pi kn/N} \tag{4}$$

where the constant $\frac{1}{\sqrt{N}}$ normalizes the power N is the subcarrier number and $X(k)$ is the modulated input symbols.

Cyclic prefix (CP) of length N_c is added at the begining of the frame which must be greater than the maximum channel delay spread then the composite symbols are transmitted through the HF channel. In order to eliminate inter-carrier interference (ICI), this guard time includes the cyclic extended part of the OFDM symbol . Next, *Pulse Shaping Filtering* is used to reconstruct on the data symbols.

After FFT is applied at the receiver, the received signal is given by:

$$\begin{aligned} Y[k] &= \sum_{n=0}^{N-1} y[n] e^{-2\pi kn/N} \\ &= \sum_{n=0}^{N-1} \left\{ \sum_{m=0}^{\infty} h[m] \left\{ \tfrac{1}{N} \sum_{n=0}^{N-1} X[i] e^{j2\pi i(n-m)/N} \right\} \right\} e^{-j2\pi kn/N} + Z[k] \\ &= \sum_{n=0}^{N-1} \left\{ \left\{ \sum_{m=0}^{\infty} h[m] e^{-j2\pi kn/N} \right\} X[i] \sum_{n=0}^{N-1} e^{j2\pi i(n-m)/N} \right\} e^{-j2\pi kn/N} + Z[k] \end{aligned}$$

$$Y[k] = \mathrm{H}[k]\mathrm{X}[k] + \mathrm{Z}[k] \tag{5}$$

where $\mathrm{X}[k]$ denotes the kth subcarrier frequency components transmitted symbol, $Y(k)$ is received symbol , $\mathrm{H}[k]$ is channel frequency response and $\mathrm{Z}[k]$ is noise in frequency domain, respectively.

At the receiver, after passing to discrete-time domain through A/D converter and pulse shaping filter, CP-based ML synchronization is applied to compansate the Carrier Frequency Offset (CFO) which is mentioned at section IV then guard time is removed:

$$y[n] = \begin{cases} x(k+M) & -M < k < 0 \\ x(n) & 0 \le k \le N-1 \end{cases} \tag{6}$$

where N is the subcarrier, M is CP length, y_n received signal that have guard interval insertion.

Then y_n is received to DFT block for the following operation:

$$\begin{aligned} Y[k] &= DFT\{y(n)\}, \;\; k, n = 0, 1, ...N-1 \\ &= \tfrac{1}{N} \sum_{n=0}^{N-1} y(n) e^{-j2\pi kn/N} \end{aligned} \tag{7}$$

Next *Least Square* estimated $\hat{H}^p_{LS}[k] = \frac{Y^p[k]}{X^p[k]}$ is obtained by extracting the pilot signals $Y^p[k]$. The interpolated $\hat{H}[k]$ for all data subcarriers is obtained in MMSE channel estimation. Then, in the Frequency domain equalization (FDE) block the transmitted data is equalized by MMSE equalizer as below:

$$\hat{X}_n = IDFT\{Y_k C_k\} = y_n \otimes c_n \tag{8}$$

where C_k represents the equalizer correction term, which is computed according to the FDE as follows:

- MMSE Equalizer:

$$C_k = \frac{\hat{H}^*_{DFT}}{\left|\hat{H}_{DFT}\right|^2 + (E_b/N_o)^{-1}} \tag{9}$$

where $(.)^*$ denotes conjugate. MMSE equalizer in (9) makes an optimum trade-off between noise enhancement and channel correction term, while using the signal-to-noise ratio (SNR) value [4]. Finally, the binary information data is obtained back in 16-QAM modulation and turbo decoding respectively.

B. SC-FDE System

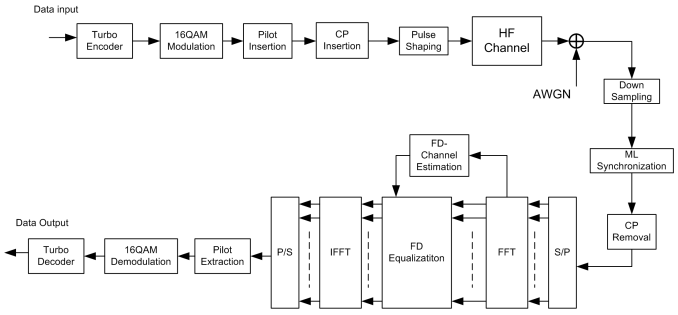

Fig. 5. SC-FDE Structure

OFDM and SC-FDE are similar in many ways. However there are explicit differences that makes the two systems perform differently. As shown at Fig.5, the main difference between OFDM and SC systems is the placement of the IDFT block. In SC systems, it is placed at the receiver side to transform the frequency domain equalized signals, thus compansating for channel distortion, bringing back to the time domain [3]. All the other blocks are formed with the same manner like OFDM system at the both sides of the transmission.

In the OFDM system, symbols are exposed to an additional transformation by using the IDFT, $x(n) = IDFT\{X[k]\}$,

but in the SC-FDE system no transformation is used. The frame of SC-FDE is transmitted during the time instant after the Turbo encoder, 16-QAM modulation, pilot insertion and CP insertion are applied respectively and the receiver maps received data into the frequency domain in order to equalize. When the channel delay spread is large it is more efficient computationally to equalize in frequency domain. In addition, SC-FDE has better behavior when used with non-linear power amplifiers.

IV. Channel Estimation & Synchronization

A. Channel Estimation

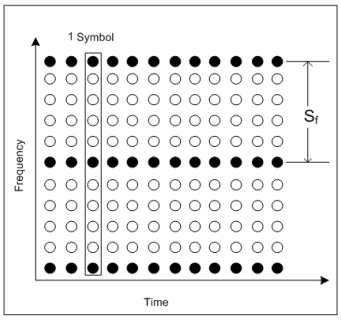

Fig. 6. Comb-type Pilot Arrangement

Comb-type pilot arrangment is shown at Fig. 6 which is used for frequency domain interpolation to estimate channel frequency response that is the Fourier transform of the channel impulse response [9,10]. In Comb-type pilot arrangement, every OFDM and SC symbol has pilot tones where are periodically located at the each subcarriers. Notice that S_f the periods of pilot tones in frequency domain must be placed in the coherence bandwidth. The coherence bandwidth is determined by an inverse of the *maximum delay spread* $\sigma_{\max}$. The pilot symbol period is shown as following inequality:

$$S_f = \frac{1}{\sigma_{\max}} \tag{10}$$

Let consider the $\hat{H}_{LS} = X^{-1}Y \triangleq \tilde{H}$, using the weight matrix *W* channel estimate $\hat{H} \triangleq W\tilde{H}$ is defined and MSE of the channel estimate is calculated as below :

$$J(\hat{H}) = E\left\{\| e\|^2\right\} = E\left\{\| H - \hat{H}\|^2\right\} \tag{11}$$

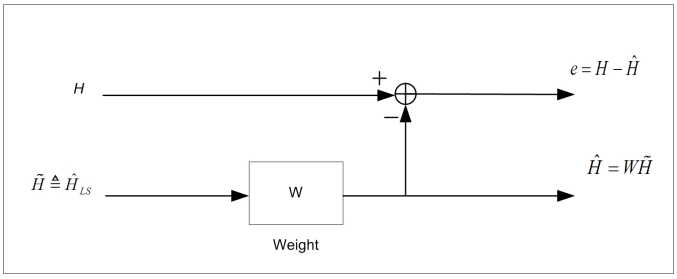

Fig. 7. MMSE Channel Estimation

MMSE estimation method shown in Fig. 7 finds a better estimate that minimizes the MSE in (11). For the derivation of MMSE channel estimation, the crosscorrelation $R_{e\tilde{H}}$, error vector *e* with channel estimate $\tilde{H}$ is forced to zero.

$$\begin{aligned} R_{e\tilde{H}} &= E\left\{e\tilde{H}^H\right\} \\ &= E\left\{(H-\hat{H})\tilde{H}^H\right\} \\ &= E\left\{(H-W\tilde{H})\tilde{H}^H\right\} \\ &= E\left\{H\tilde{H}^H\right\} - WE\left\{\tilde{H}\tilde{H}^H\right\} \\ &= R_{H\tilde{H}} - WR_{\tilde{H}\tilde{H}} = 0 \end{aligned} \tag{12}$$

where $(.)^H$ *Hermitian* operator. Solving eqaution (12) for *W* yields:

$$W = R_{H\tilde{H}}R_{\tilde{H}\tilde{H}}^{-1} \tag{13}$$

Using (13) the MMSE channel etimate follows as:

$$\hat{H} = W\tilde{H} = R_{H\tilde{H}}R_{\tilde{H}\tilde{H}}\tilde{H} \tag{14}$$

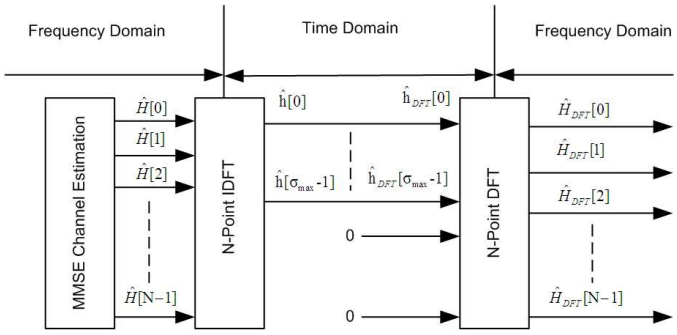

Fig. 8. DFT-based Channel Estimation

Fig. 8 shows the block diagram of DFT-based channel estimation, given the MMSE channel estimation. An important point is that $\sigma_{\max}$ must be known formerly to remove the effect of noise outside the channel delay. Taking the IDFT of the MMSE channel estimate $\hat{H}$ to get in the time domain, that the coefficients contain the noise are ignored with zero padding and then transform the remaining $\sigma_{\max}$ elements back to the frequency domain to achieve $\hat{H}_{DFT}$. Finally $\hat{H}_{DFT}$ is used in (9) at the Frequency Domain MMSE Channel Equalizer block.

B. Channel Synchronization

In general, there are two types of distortion related with the carrier signal. One is the Phase Noise due to the Voltage Control Ossilator (VCO) and the other is Carrier Frequency Offset (CFO) caused by Doppler Frequency shift f_d. Let define the normalized CFO, ε, as a ratio of the CFO to subcarrier spacing Δ_f is shown as:

$$\varepsilon = \frac{f_d}{\Delta_f} \tag{15}$$

where f_d is the Doppler Frequency.

CP-based channel synchronization estimates the time and carrier-frequency offset. This algorithm exploits the cyclic

prefix preceding the OFDM and SC symbols, thus reducing the need for pilots. The received data in the time domain $e^{j2\pi\varepsilon k/N}$, where ε denotes the difference in the transmitter and receiver oscillators as a fraction of the inter-carrier spacing , that is calculated in (15). Notice that all subcarriers are effected by the same shift ε is shown as:

$$r(k) = s(k-\theta)e^{j2\pi\varepsilon k/N} + n(k) \tag{16}$$

where $r(k)$ is the received data, $s(k-\theta)$ is the unknown arrival time transmitted signal and $n(k)$ is the AWGN. Hence $r(k)$ contains information about the time offset θ and carrier offset ε. From the observation shown in Fig. 9 that the estimation of frequency offset and the estimation of timing offset are calculated as below:

$$\begin{aligned} \gamma(m) &\triangleq \sum_{k=m}^{m+L-1} r(k)r^*(k+N) \\ \Phi(m) &\triangleq \tfrac{1}{2}\sum_{k=m}^{m+L-1} |r(k)|^2 + |r(k+N)|^2 \end{aligned} \tag{17}$$

where L is the CP length and m is the index of samples [11,12]. Notice from Fig. 9 that peaks of the timing estimate, six frame are obtained from the observation interval.

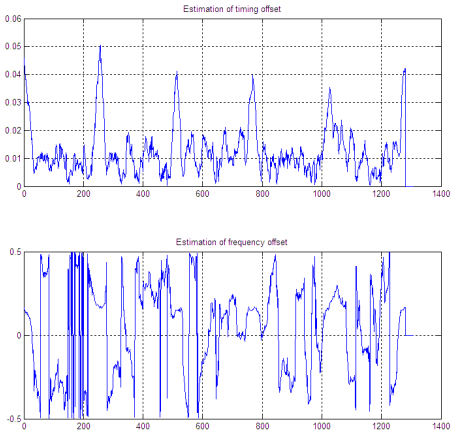

Fig. 9. STO and CFO estimates

Next, the index values of the peaks of the timing estimate gives the estimates of carrier frequency offsets $\hat{\varepsilon}$ values:

$$\hat{\varepsilon} = \hat{\gamma}(maxindexvalues(\hat{\Phi}(m))) \tag{18}$$

Finally, these estimates are used in channel synchronization block to compansate the carrier frequency offset as:

$$\hat{s}(k) = r(k) \cdot e^{-j2\pi\hat{\varepsilon}k/N} \tag{19}$$

where $\hat{s}(k)$ is the synchronized signal.

V. Numerical Results

In this section, BER performance of the proposed systems for CFO, STO and phase noise are shown. The simulation parameters are compliant to the wideband HF channel model: 24 KHz bandwidth, 16 QAM constellation, 256 subcarriers, 210 occupied sub-carriers, 16 cyclic prefix length and pilot tone number is equal to 30. The code rate of the turbo code is $1/3$, the interleaveris 512 block interleaver and 10-iteration log-MAP decoding is used.

In all of the simulations, normalized frequency offset of each system is a constant value between 0.1 and 0.5. For the channel model, multipath fading channel is used which can be modelled as a tapped-delay line with $L_{ch} = 3$ delay taps. The channel gains of the taps are [0 -3 -8] dB and the bandwidth of the HF channel is 24KHz.

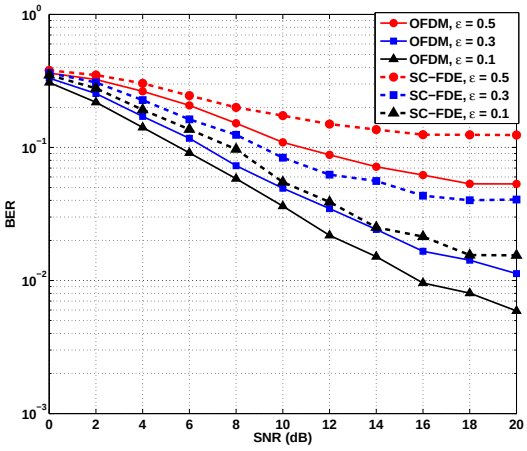

Fig. 10. BER performance versus SNR in dB paramterized by CFO.

In the first simulation, the effect of CFO is analyzed. Hence, normalized CFO, ε, is calculated from Equation (15). In this simulation, channel delay spread and phase noise are neglected. As can be seen from the figure 10, as the frequency offset of the channel increases, BER performances decrease as well. This is because of the way that CFO increments the ICI without the CP-based channel synchronization. Both OFDM and SC-FDE systems experience the impacts of severe frequency-selective fading channels even so there are certain contrasts between the performance of their decoders. For lower code rates such as $R = 1/3$ Turbo code; OFDM out-performs SC-FDE. For SC-FDE, the noise amendment loss increases with the average input SNR. When the channel is ineffective and the SNR is high, the equalizer tries to invert the nulls and as a result, the noise in these ineffective locations is amplified. Conversely, OFDM combines the useful energy across all subcarriers through turbo-coding and interleaving.

In the second simulation, the effect of the channel delay spread, that is modelled with zero padding in each propagation path is analyzed. It is assumed that no CFO and phase noise exist. The simulation results are showed in the range of 3ms to 10ms channel delay spread. The $R = 1/3$ rate, 4

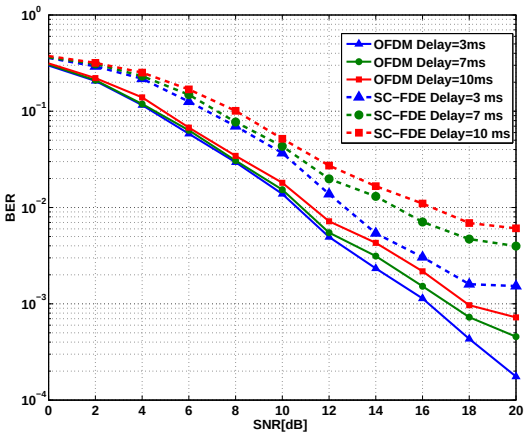

Fig. 11. BER performance versus SNR in dB parametrized by STO.

state (7,5) convolutional turbo encoder has d_{free}. Therefore, a coded OFDM system with this turbo code can achieve a diversity order of 5 without implementing any additional transmit/receive antennas, or using any other diversity techniques. Hence, especially when the channel order is larger, lower rate codes are required to achieve full diversity in OFDM systems. When this is the case, OFDM gives better performance than SC-FDE sytem because of the reduced effect of ISI.

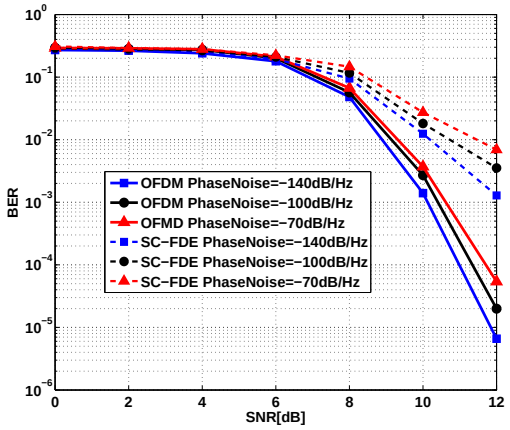

Fig. 12. BER performance versus SNR in dB parametrized by phase noise level in dBc/Hz.

For the third simulation, the effect of random fluctuations in the phase of a waveform due to the VCO at the -140dBc/Hz, -100dBc/Hz, and -70dBc/Hz values is analyzed. For all simulations it can be seen that increasing the CFO, STO and phase noise effect clearly decreases the system performances especially for SC-FDE.

VI. Conclusion

In this paper, the performances of the turbo-coded SC and OFDM systems using FDE, MMSE channel estimation, CP-based synchronization over the Wideband Vogler-Hoffmeyer HF channel are simulated. The performance of the proposed systems were compared under only CFO, STO and phase noise effects. The simulation results confirm that turbo-coded OFDM performs significantly better than turbo-coded SC-FDE in HF channel model with the large diversity.

References

[1] S. B. Weinstein, et al., ”Data Transmission by Frequency-Division Multiplexing Using the Discrete Fourier Transform”, IEEE transactions on communication technology, vol. 19, no. 5, Oct. 1971.

[2] D. Falconer, S. L. Ariyavistakul, A. Benyamin-Seeyar, and B. Edison, Frequency domain equalization for single carrier broadband wireless systems”, IEEE Commun.Mag., pp.58-66, Apr. 2002.

[3] Fabrizio Pancaldi, et al., ”Single-Carrier Frequency Domain Equalization”, IEEE Signal Processing Magazine, Volume:25, Issue: 5, pp. 37-55 Sep. 2008

[4] Emad S. Hassa, Xu Zhu, Said E. El-Khamy, et al., ”Enhanced Performance of OFDM and Single-Carrier Systems Using Frequency Domain Equalization and Phase Modulation”, 26^{th} National Radio Science Conference (NRSC2009), pp.1-10, March 2009.

[5] C. C. Watterson, J. R. Juroshek, W. D. Bensema, Experimental Confirmation of an HF Channel Model, IEEE Trans. On Comm. Tech., Vol. COM-18, No. 6, Dec. 1970.

[6] ITU, HF Ionospheric Channel Simulators, CCIR Report 549-2, Recommendations and Reports of the CCIR, Vol. III, pp. 59-67, Geneva

[7] J. A. Hoffmeyer, L. E. Vogler, ”A New Approach to HF Channel Modeling and Simulation”, Military Communications Conference, MILCOM ’90, pp.1199-1208 vol.3. 1990.

[8] Yang Guo; Ke Wang, A Real-Time Software Simulator of Wideband HF Propagation Channel, ICCSN 09 International Conference on Communication Software and Networks, 2009, pp.304308, 27-28 Feb.2009.

[9] Yushi Shen and Ed Martinez, Channel Estimation in OFDM Systems, Free scale Semiconductor, AN3059 Inc., 2006, August 2008.

[10] Sinem Coleri, Mustafa Ergen, Anuj Puri, and Ahmad Bahai, Channel Estimation Techniques Based on Pilot Arrangement in OFDM Systems IEEE Transactions on Broadcasting, vol. 48, NO. 3 Sep-2002.

[11] J.-J.van de Beek, O. Edfors, M. Sandell, S. K. Wilson, and P. O. Börjesson, ” On Channel Estimation in OFDM Systems”, Proceeding of th IEEE Vehicular Technology Conference, vol.2, pp.815-819,july 1995

[12] Magnus Sandell, Jan-Jaap van de Beek, Per Ola Börjesson,”Timing and frequency synchronization in OFDM systems using the cyclic prefix”,International Symposium on Synchronization, pp.16-19,Dec 1995.